Downloaded from UvA-DARE, the institutional repository of the University of Amsterdam (UvA)
http://hdl.handle.net/11245/2.39542

File ID	uvapub:39542
Filename	171003y.pdf
Version	unknown

SOURCE (OR PART OF THE FOLLOWING SOURCE):

Type	article
Title	Magnetization studies of RMn6Ge6-xGax single crystals (R = Sc, Y, Gd-Lu; 0.63 <= x <= 1.00)
Author(s)	L. Zhang, J.C.P. Klaasse, E.H. Brück, K.H.J. Buschow, F.R. de Boer, S. Yoshii, K. Kindo, C. Lefevre, G. Venturini
Faculty	FNWI: Van der Waals-Zeeman Institute (WZI)
Year	2004

FULL BIBLIOGRAPHIC DETAILS:
http://hdl.handle.net/11245/1.229281

Copyright

It is not permitted to download or to forward/distribute the text or part of it without the consent of the author(s) and/or copyright holder(s), other than for strictly personal, individual use, unless the work is under an open content licence (like Creative Commons).

UvA-DARE is a service provided by the library of the University of Amsterdam (http://dare.uva.nl)
(pagedate: 2014-11-16)

Magnetization studies of $RMn_6Ge_{6-x}Ga_x$ single crystals (R=Sc, Y, Gd–Lu; $0.63 \leqslant x \leqslant 1.00$)

L. Zhang, J. C. P. Klaasse, E. Brück, K. H. J. Buschow, and F. R. de Boer
Van der Waals-Zeeman Instituut, Universiteit van Amsterdam, Valckenierstraat 65, 1018 XE Amsterdam, The Netherlands

S. Yoshii and K. Kindo
Research Center for Materials Science at Extreme Conditions, Osaka University, 1-3 Machikaneyama, Toyonaka, Osaka 560-8531, Japan

C. Lefèvre and G. Venturini
Laboratoire de Chimie du Solide Minéral, Université Henri Poincaré-Nancy I, Associé au CNRS (UMR 7555), B.P. 239, 54506 Vandoeuvre les Nancy Cedex, France
(Received 4 May 2004; published 21 December 2004)

The magnetic properties of single crystals of rare-earth compounds of composition $RMn_6Ge_{6-x}Ga_x$ ($x \approx 1$) have been studied. In these compounds, the Mn sublattice orders ferromagnetically with a preferred moment direction perpendicular to the c axis. In the compounds in which also the R component carries a magnetic moment, the latter couple antiparallel to the Mn moments. Upon cooling from room temperature to cryogenic temperatures, the R-sublattice anisotropy becomes the dominant contribution to the total magnetocrystalline anisotropy, which leads to a spin-reorientation transition at intermediate temperatures for R=Tb−Yb. At low temperatures, the preferred moment directions are characterized by an easy axis for R=Tb, Er, Tm, and Yb and by an easy cone for R=Dy and Ho. A satisfactory account of the observed preferred moment directions has been given in terms of crystal-field theory. Measurements of the magnetization in the main crystallographic directions have been made in high magnetic fields, up to about 55 T. The interplay between the antiferromagnetic intersublattice R-Mn coupling and the magnetocrystalline anisotropy leads to field-induced magnetic phase transitions which are particularly pronounced in the compounds with Ho, Er and Tm.

DOI: 10.1103/PhysRevB.70.224425 PACS number(s): 75.50.Gg

I. INTRODUCTION

The hexagonal $HfFe_6Ge_6$-type RMn_6Ge_6 compounds, with R=Sc, Y, or one of the rare-earth elements, have been extensively studied during the last decade.[1–5] They display a wide variety of magnetic behavior originating from the different Mn-Mn, R-Mn and R-R exchange interactions and/or from contributions to the magnetocrystalline anisotropy due to both the R and the Mn sublattice. An analysis of the magnetic properties of all these materials is seriously hampered because the Mn moments form two separate sublattices whose moments adopt a mutually canted orientation. However, recent investigations of $RMn_6Ge_{6-x}Ga_x$ ($0 \leqslant x \leqslant 2$) solid solutions have revealed interesting properties.[6–8] At a fairly modest Ga-substitution level, it has been observed that the Mn moments become collinear in all pseudoternary compounds. This feature leads to the stabilization of a ferrimagnetic moment arrangement for all compounds in which R is magnetic, offering the opportunity to easily check the evolution of the magnetocrystalline anisotropy as a function of the R element. In the present paper, we present results of magnetization measurements performed on single-crystalline samples in fields up to about 55 T.

II. EXPERIMENTAL

The $RMn_6Ge_{6-x}Ga_x$ crystals for the present study have been obtained by a flux method. A mixture of RMn_6Ge_6, obtained by induction melting, and elemental Ge is compacted into pellets and put into a silica tube with a large amount of In and Ga metal giving rise to the overall atomic ratio $RMn_6Ge_9Ga_{27}In_{31}$. A quartz-wool stopper is introduced in the silica tube which is sealed under argon (267 mbar). The tube is placed in a furnace and quickly heated to 1273 K (50 K/h) where it remains during 24 h. The furnace is then slowly cooled down to 1223 K (6 K/h), heated again up to 1263 K at the same rate and finally slowly cooled down to 873 K in 65 h. The tube is quickly removed from the furnace, inverted and centrifugated manually using a David's sling device. After this treatment, the single crystals remain on the quartz wool stopper and the In-Ga flux lies at the bottom of the tube. The remaining flux on the crystals is removed using diluted hydrochloric acid. This method produces well shaped hexagonal prisms with masses of 1–5 mg. Except for the Sc compound, their mean size decreases with the rare-earth atomic size. Some of the crystals have been ground and analyzed by x-ray diffraction using a Guinier camera (CoKα). The Ga content has been checked at the Service Commun d'Analyse par Microsondes Electroniques de l'Université de Nancy I-Henri Poincaré using an SX50 electron probe.

The thermal variation of the magnetization has been measured in a DSM8 magneto-susceptometer in an applied field of 0.1 T in the temperature range 5–450 K. The Curie temperature and the spin-reorientation-transition temperature have been taken at the maximum of the first derivate dM/dT. Magnetization measurements in fields up to 7 T in the temperature range 6–300 K have been performed in the SQUID magnetometer at the Service Commun de Magnétisme de l'Université de Nancy I-Henri Poincaré.

 ©2004 The American Physical Society

TABLE I. Cell parameters, Ga contents and magnetic properties of $R\mathrm{Mn}_6\mathrm{Ge}_{6-x}\mathrm{Ga}_x$ crystals (R=Sc, Y, Gd-Lu).

R	x	a (Å)	c (Å)	c/a	T_C (K)	T_{sr} (K)	$M_S \perp c$ $(\mu_B)\parallel$	$M_S \parallel c$ (μ_B)	M_S[a] (μ_B)	θ_{cone}[c] (°)	μ_{Mn}[b] (μ_B)
Sc	0.82	5.162(2)	8.151(5)	1.5791	386	-	9.85	0	9.85	90	1.64
Y	0.83	5.226(3)	8.214(6)	1.5719	350	-	11.05	0	11.05	90	1.84
Gd	0.81	5.236(3)	8.237(5)	1.5731	413	-	4.50	0	4.50	90	1.92
Tb	0.78	5.228(2)	8.221(5)	1.5725	408	196	0	2.34	2.34	0	1.89
Dy	0.83	5.228(3)	8.218(6)	1.5719	390	260	1.16	0.89	1.46	53	1.91
Ho	0.95	5.221(3)	8.217(5)	1.5738	372	143, 260	0.79	1.15	1.40	34	1.90
Er	0.91	5.212(3)	8.206(5)	1.5744	361	186	0	2.07	2.07	0	1.85
Tm	0.87	5.209(3)	8.208(5)	1.5757	352	45	0	4.05	4.05	0	1.84
Yb	0.63	5.198(3)	8.182(5)	1.5741	358	210	0	8.77	8.77	0	2.13
Lu	1.00	5.199(3)	8.202(5)	1.5776	353	-	11.15	0	11.15	90	1.86

[a] M_s represents spontaneous magnetization.
[b] Calculated as $\mu_{Mn}=1/6(M_S+\mu_R^{3+})$, assuming the theoretical R^{3+} free-ion value.
[c] $\theta_{cone}=\arctan(M_s \perp c/M_s \parallel c)$.

High-field magnetization studies have been carried out in the High-Field Installation at the University of Amsterdam in fields up to 38 T with pulse duration of about 0.5 s and in the Research Center for Materials Science at Extreme Conditions at Osaka University in pulsed fields up to 55 T with a pulse duration of usually 8 ms and in some cases 20 ms. The magnetic fields were applied along the *a*-axis, the *b*-axis and the *c*-axis as depicted later in Fig. 7(a), where they are perpendicular to each other. Because of the rather high residual resistivity of the $R\mathrm{Mn}_6(\mathrm{Ge},\mathrm{Ga})_6$ samples, the eddy-current effect is negligibly small in the present pulsed-field measurements. This is confirmed by the fact that the field-decreasing process well coincides with the field-increasing process.

III. EXPERIMENTAL RESULTS

A. Crystal structure

Analysis of the Guinier patterns shows that all studied crystals are isotypic with the hexagonal $\mathrm{HfFe}_6\mathrm{Ge}_6$ structure. The Ga contents and the lattice parameters are presented in Table I. Although similar initial atomic concentrations have been used for the synthesis, the final Ga contents in the crystals may slightly vary. This is inherent in the presently used type of synthesis method and is particularly pronounced for the Yb compound, a feature which might be related to a possible abnormal valence of this element. For the other crystals, the Ga concentrations range between $x=0.78$ and $x=1.00$ with an average value $x=0.87$. Previous studies on polycrystalline $\mathrm{LuMn}_6\mathrm{Ge}_{6-x}\mathrm{Ga}_x$ samples have shown that the magnetic properties of the Mn sublattice drastically vary only for small Ga concentrations, in the range $x=0.0$ to 0.6.[8] However, for the Ga concentrations considered in the present paper, the ferromagnetic state is fairly stable (reached in $\mathrm{LuMn}_6\mathrm{Ge}_{6-x}\mathrm{Ga}_x$ for x close to 0.80) and persists for larger Ga concentrations, giving rise only to a small decrease of the Curie temperature ($\Delta T_c/\Delta x \approx -67$ K).[7] Therefore, in the studied Ga-concentration range, the variation of the concentration measured in the crystals should not drastically influence the magnetic properties of the Mn sublattice and the differences in magnetic properties observed for the compounds studied should reflect the influence of the R element. The single-crystal refinement of the structure of $\mathrm{ErMn}_6\mathrm{Ge}_{5.1}\mathrm{Ga}_{0.9}$ has been reported elsewhere.[9] Er is positioned at 1*a* (0, 0, 0), Mn at 6*i* (1/2, 0, $z=0.2484$), Ge_1 at 2*c* (1/3, 2/3, 0), Ge_2 at 2*d* (1/3, 2/3, 1/2) and Ge_3 at 2*e* (0, 0, $z=0.3462$). An analysis of the atomic coordinates suggests that the Ga atoms are mainly located at the Ge_2 site in fair accordance with neutron-diffraction results.[7]

B. Magnetic properties

1. Thermal variation of the magnetization in low magnetic field

The thermal variation of the magnetization in 0.1 T between 5 and 450 K is shown in Figs. 1 and 2 for all studied $R\mathrm{Mn}_6(\mathrm{Ge},\mathrm{Ga})_6$ compounds and the results are summarized in Table I. For the compounds with the nonmagnetic elements Sc, Y and Lu, one observes a decrease of the ordering temperature with increasing atomic size of these elements (Fig. 3). Most likely, this dependence is related to the corresponding increase of the Mn-Mn interatomic distances. An opposite dependence is observed for the compounds containing R elements that carry a magnetic moment. The ordering temperature decreases on going from the Gd compound to the Yb compound, thus accounting for the dominant influence of the R-Mn interaction that decreases from Gd to Yb. The $R\mathrm{Mn}_6\mathrm{Ge}_{6-x}\mathrm{Ga}_x$ compounds in which R does not carry a magnetic moment (R=Sc, Y, Lu), as well as the Gd compound possess easy-plane anisotropy in the whole ordered range (Fig. 1). The magnetization vs field curves recorded at 10 and 300 K enable a rough determination of the anisotropy of the Mn sublattice at these temperatures. Results obtained by means of the Sucksmith and Thompson method[11] are reported in Table II. The anisotropy type is determined by the cone angle, i.e. the easy axis for $\theta_{cone}=0°$, the easy plane for $\theta_{cone}=90°$ and the easy cone in the other cases.

The temperature dependence of the magnetization of the compounds in which also the R atom carries a moment (R

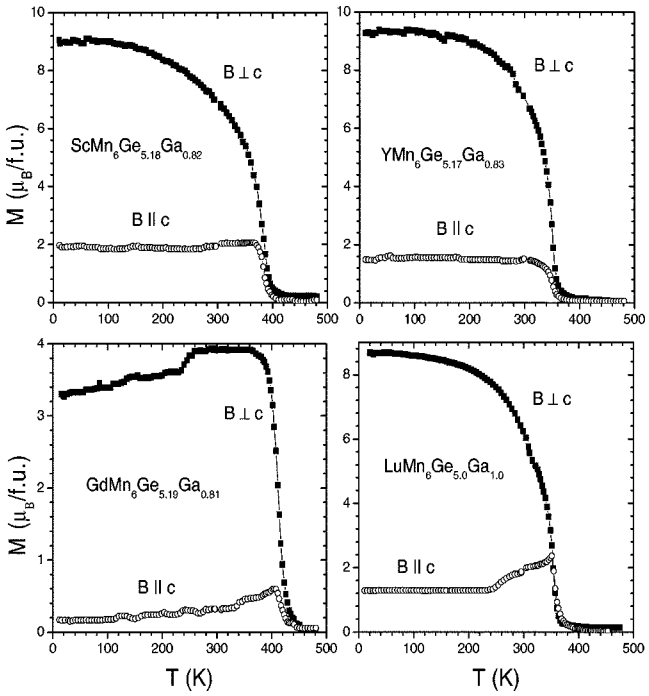

FIG. 1. Thermal variation of the magnetization of RMn$_6$Ge$_{6-x}$Ga$_x$ compounds with R=Sc, Y, Gd and Lu in an applied field of 0.1 T. No correction has been made to take into account the effect of the demagnetizing field

=Tb-Yb) is displayed in Fig. 2. The results indicate an easy-plane arrangement at ambient temperature and a spin-reorientation transition at lower temperature. For the Tb, Er and Tm compounds, the magnetization measured perpendicular to the c-axis drastically decreases below the spin-reorientation-transition temperature whereas this transition is more gradual for the Yb compound. At low temperature, the Dy and Ho compounds still exhibit nonzero spontaneous magnetization in the direction perpendicular to the c-axis, indicating a conical structure which is in fair accordance with neutron-diffraction results.[6,10] An additional transition is observed in the magnetization curve of the Ho compound measured perpendicular to the c-axis, in agreement with the neutron-diffraction results that show that at 175 K the moment direction is close to the c-axis.[10]

The compounds that have easy-axis anisotropy at low temperature display rather large coercive fields ($\mu_0 H_c$ =1.1 T for Tb, 0.9 T for Er, 0.2 T for Tm and 0 T for the Yb compound). The magnitude of the coercive field is rather well related to the temperature of the spin-reorientation transition. The Yb compound does not exhibit a large coercive field, in spite of its high transition temperature.

The Mn moments deduced from the spontaneous magnetization, assuming the R atoms to possess the theoretical R^{3+} free-ion moment are presented in Table I. The spontaneous Mn moment of the Yb compound is anomalously large, indicating that Yb does not possess its full trivalent moment in this compound.

2. Field and temperature dependence of the magnetization

The magnetization of the compounds with Ho, Tm and Yb has been measured in fields up to 7 T at temperatures between 6 and 300 K. The magnetization curves of the Ho compound are shown in Fig. 4, with the applied field parallel and perpendicular to the c-axis. Between 150 and 200 K, the magnetization measured perpendicular to the c-axis clearly shows the absence of spontaneous magnetization, accounting

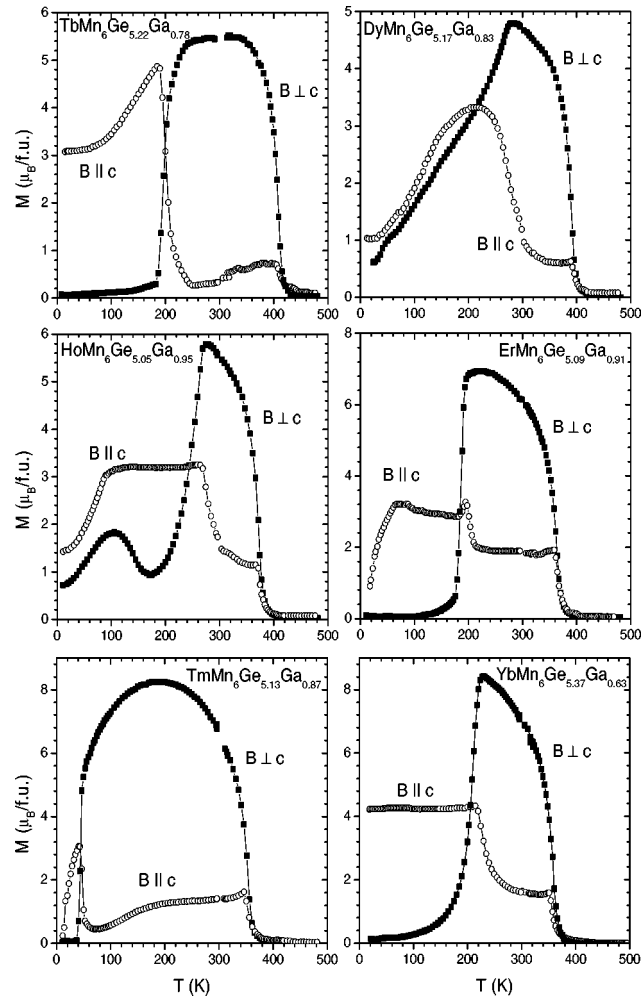

FIG. 2. Thermal variation of the magnetization of RMn$_6$Ge$_{6-x}$Ga$_x$ compounds with R=Tb−Yb in an applied field of 0.1 T. No correction has been made to take into account the effect of the demagnetizing field.

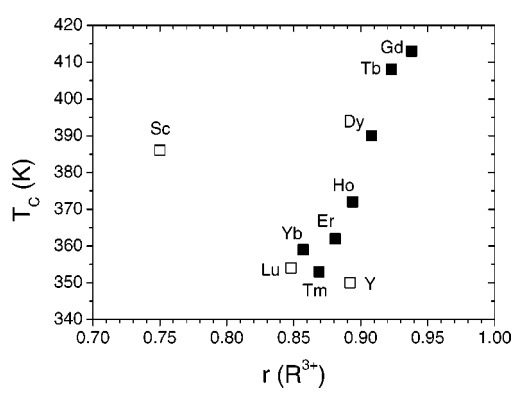

FIG. 3. Variation of the Curie temperature of RMn$_6$Ge$_{6-x}$Ga$_x$ compounds with the ionic radius of the R element.

TABLE II. Anisotropy constants of the Mn sublattice in $RMn_6Ge_{6-x}Ga_x$ compounds with R=Sc, Y, Gd, Lu.

R	T (K)	K_1^{Mn} (MJ/m^3)	K_2^{Mn} (MJ/m^3)	Anisotropy type
Sc	300	−0.10	0.02	Easy plane
	10	−0.14	0.01	Easy plane
Y	300	−0.07	0.02	Easy plane
	10	−0.22	0.01	Easy plane
Gd	300	−0.17	0.01	Easy plane
	10	−0.27	0.00	Easy plane
Lu	300	−0.08	0.01	Easy plane
	10	−0.33	0.07	Easy plane

for the occurrence of a uniaxial magnetic structure in a limited temperature range. Below 100 K, spontaneous magnetization occurs along both of the two measuring directions thus indicating a conical structure with a semi-cone angle close to 34°.

Results obtained for the Tm compound are shown in Fig. 5. Spontaneous magnetization is observed in the magnetization curves perpendicular to the c-axis above 100 K and along the c-axis only at 6 and 30 K. As seen in Fig. 5(a), at 6 K, an applied field of about 2 T is sufficient to rotate the moment into the c direction and hysteresis is involved in this process.

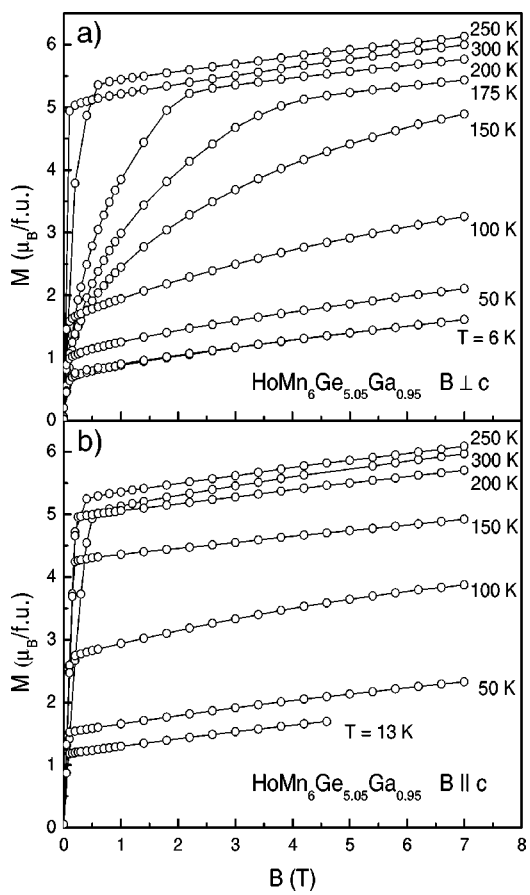

FIG. 4. Magnetic isotherms of $HoMn_6Ge_{5.05}Ga_{0.95}$, measured between 6 and 300 K; (a) perpendicular to the c-axis and (b) along the c-axis.

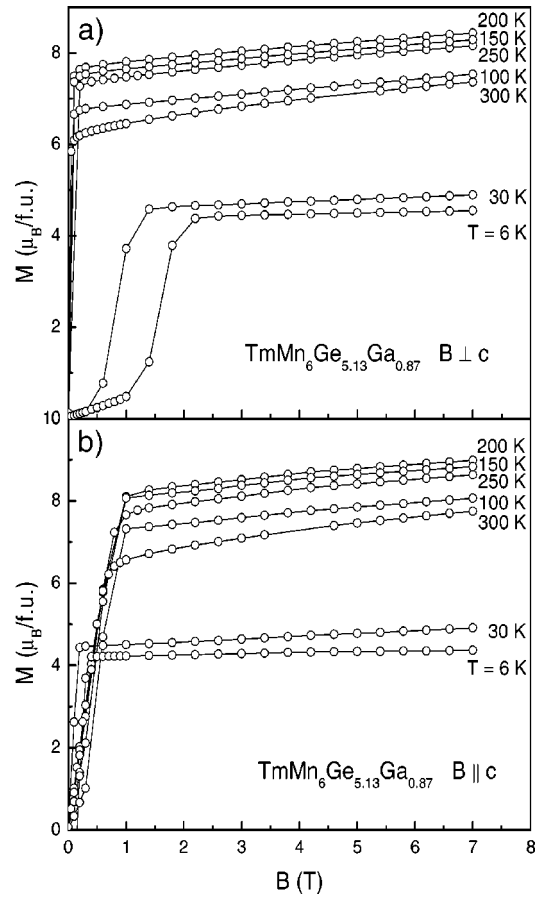

FIG. 5. Magnetic isotherms of $TmMn_6Ge_{5.13}Ga_{0.87}$, measured between 6 and 300 K; (a) perpendicular to the c-axis and (b) along the c-axis.

Figure 6 shows the results for the Yb compound. The magnetization curves recorded perpendicular to the c-axis display strong anisotropy effects below 50 K and an applied field of 7 T is not able to align the magnetic moments perpendicular to the c direction.

3. Magnetization in high magnetic fields

Magnetization measurements at 4.2 K in fields up to about 55 T have been made on the compounds with Gd, Tb, Dy, Ho, Er, Tm, Yb and Lu, of which single crystals were available of sufficient size for high-field experiments.

The magnetic isotherms measured on the Gd compound along the two principal directions are displayed in Fig. 7. The inset diagram (a) displays the defined a-, b- and c-axis in the hexagonal basal plane. Initially, the Gd-sublattice moments are antiparallel to the Mn-sublattice moments in the basal plane as schematically shown in diagram (b), with a net moment of about 4.5 μ_B/f.u. Note that in the schematic moment configuration diagrams here and hereafter the horizontal direction indicates the a-axis while the vertical direction indicates the c-axis. With field along the a-axis, a field of 47 T is still not high enough to lead to canting of the Mn and Gd moments towards each other, which could finally lead to a

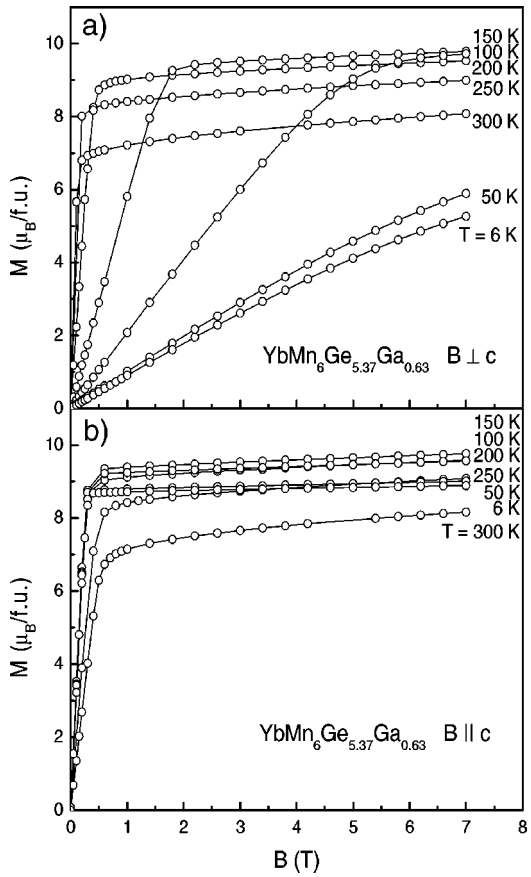

FIG. 6. Magnetic isotherms of $YbMn_6Ge_{5.37}Ga_{0.63}$, measured between 6 and 300 K; (a) perpendicular to the c-axis and (b) along the c-axis.

forced ferromagnetic arrangement. With a field along the c-axis, the linear increase of the magnetization in the beginning corresponds well to a rigid rotation of both sublattices towards the c-axis against anisotropy [diagram (c)]. A sluggish increase of magnetization from 5 T until 47 can be explained by the Gd-sublattice bending towards the magnetic field direction [diagram (d)].

Results obtained for the Tb compound are shown in Fig. 8. The initial moment arrangement is shown schematically in

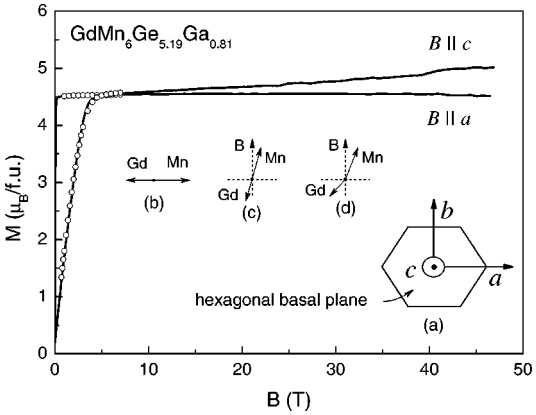

FIG. 7. Magnetization of $GdMn_6Ge_{5.19}Ga_{0.81}$, measured at 4.2 K along the a-axis and the c-axis. See the text for the inset diagrams. The symbols represent SQUID measurements for calibration.

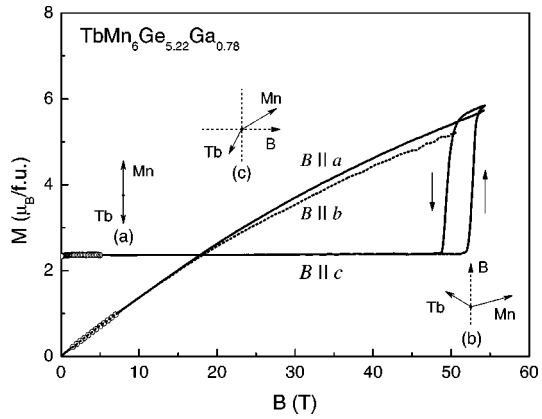

FIG. 8. Magnetization of $TbMn_6Ge_{5.22}Ga_{0.78}$, measured at 4.2 K along the a-axis, the b-axis (dotted curve) and the c-axis. The symbols represent SQUID measurements for calibration.

diagram (a), the total Mn-sublattice magnetization being larger than the Tb-sublattice magnetization. At about 52 T, when the measurement is along the c direction, there is a large jump in the magnetization, from the moment configuration in diagram (a) to the one in diagram (b). The large hysteresis indicates the typical character of the first-order magnetic transition. When the field is along the a-axis, the total moment will turn away from the c-axis, retaining the antiparallel intersublattice coupling as far as possible and bending towards the field direction [diagram (c)]. No magnetization jump is observed up to 54 T. In this connection, we note that we observed only a minor difference between the a-axis and the b-axis. Above 15 T, the shift to the lower magnetization for the b-axis, compared to the a-axis, became more pronounced with increasing magnetic fields, indicating a slightly larger energy barrier for the bending towards the b-axis.

The results for the Dy compound are displayed in Fig. 9. At about 40 T, there is a clear transition in the magnetization measured with the field applied along the c direction. One small jump around 22 T is observed in the isotherm measured along the a direction. In this compound, the moment arrangement is of the easy-cone type. Therefore, the magne-

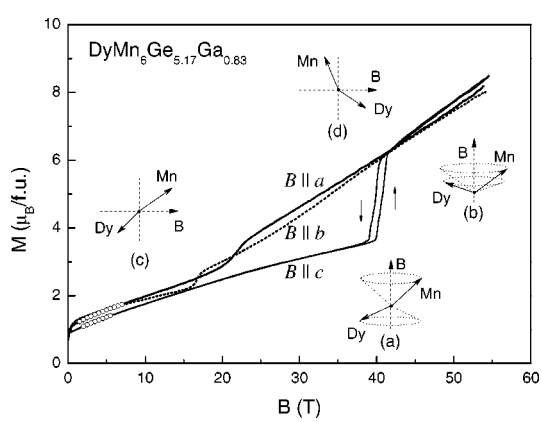

FIG. 9. Magnetization of $DyMn_6Ge_{5.17}Ga_{0.83}$, measured at 4.2 K along the a-axis, the b-axis (dotted curve) and the c-axis. The symbols represent SQUID measurements for calibration.

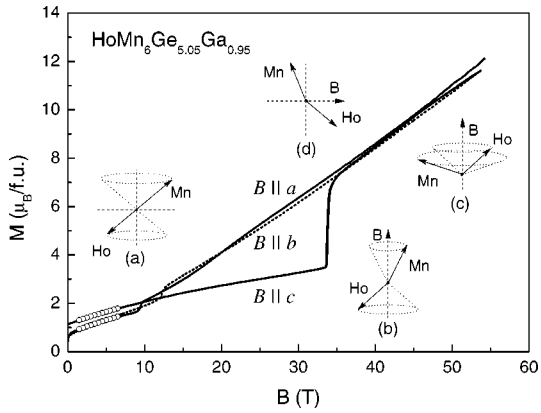

FIG. 10. Magnetization of $HoMn_6Ge_{5.05}Ga_{0.95}$, measured at 4.2 K along the *a*-axis, the *b*-axis (dotted curve) and the *c*-axis. The symbols represent SQUID measurements for calibration.

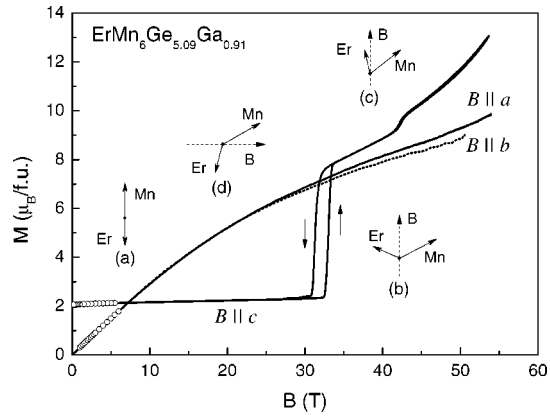

FIG. 11. Magnetization of $ErMn_6Ge_{5.09}Ga_{0.91}$, measured at 4.2 K along the *a*-axis, the *b*-axis (dotted curve) and the *c*-axis. The symbols represent SQUID measurements for calibration.

tization measured along both directions increases strongly at the beginning. Bearing in mind that the Mn-sublattice anisotropy is much smaller than the Dy-sublattice anisotropy and that the Mn and Dy moments tend to couple antiparallel as far as possible, we interpret the jump of the magnetization at 40 T as a moment rearrangement from the configuration in diagram (a) to the one in diagram (b). The increase of the magnetization above the jump can be attributed to a gradual bending of the Mn- and the Dy-sublattice moments into the direction of the applied field. In the small magnetization jump in the isotherm measured in the direction along the a axis, the change in magnetic moment arrangement affects the antiparallel coupling between the two sublattices only slightly, as can be seen when comparing diagram (c) with diagram (d). The smallness of this jump probably originates from the fact that, due to the initial cone arrangement, there is not much change in magnetization between the moment arrangements displayed in diagrams (c) and (d). The small jump in the direction along the b-axis starts at a lower field 16 T than that 20 T along the *a*-axis. This can be interpreted by a smaller anisotropy energy along the *b*-axis than along the *a*-axis for the Dy magnetic sublattice.

Like in the Dy compound, the moment arrangement is also of the easy-cone type in the Ho compound, so that the two magnetic isotherms for the Ho compound shown in Fig. 10 exhibit close resemblance to the ones for the Dy compound. Starting from a moment configuration corresponding to diagram (a), the magnetization measured with the field applied along the *c* direction exhibits a jump at 33 T from the moment arrangement depicted in diagram (b) to that in diagram (c). In the Ho compound, the intersublattice-coupling strength, tending to keep the Ho and Mn moments antiparallel, is smaller than in the Dy compound which explains why the field of the magnetization jump is smaller in the former 33 T than in the latter 40 T. There is a small magnetization jump around 10 T in the isotherm measured with the field applied along the *a* direction, which corresponds to an eventual change in moment arrangement as displayed in diagrams (a) and (d). Again just like in the Dy compound, the magnetization measured along the *b*-axis is only slightly different from that along the *a*-axis. However, the critical field corresponding to the small jump along the *b*-axis in the Ho compound shifts toward a higher field instead of to a lower one as in the Dy compound, indicating a smaller anisotropy energy along the a-axis than along the *b*-axis.

The results for the Er compound are shown in Fig. 11. Like in the Tb compound, the easy magnetization direction is along *c* and we will discuss the results of the corresponding isotherm first. The moment arrangement in low fields is as shown schematically in diagram (a), the total Mn-sublattice magnetization being larger than the Er-sublattice magnetization. At about 32 T, there is a large jump in the magnetization, from the moment configuration in diagram (a) to the one in diagram (b). The lower transition field 32 T here, compared to that 52 T in Tb compound can be explained by a lower intersublattice-coupling strength in the Er compound. A second, smaller magnetization jump, presumably to the configuration in diagram (c), is observed at about 42 T. Above this minor jump, the Er and Mn moments gradually bend into the direction of the applied field. In the isotherm obtained when the field is applied along the hard direction, i.e. the *a*-axis, no magnetization jump is observed up to 56 T. In this magnetization process, the total moment will turn away from the *c*-axis, retaining the antiparallel intersublattice coupling as far as possible as depicted in diagram (d). Eventually, the two sublattice moments will be oriented in the direction of the applied field. Similar to the Tb compound, the magnetization curve for the *b*-axis starts shifting towards lower values from that for the *a*-axis at 25 T and the deviation becomes larger in higher fields. This deviation might be recovered by an additional step in the isotherm for the *b*-axis at an even higher field than that of the current experiment.

The magnetic isotherms measured for the Tm compound in the three main crystallographic directions are shown in Fig. 12. If the field is applied along the *c* direction, which is the easy magnetization axis, the magnetization slightly increases in the range up to about 20 T which is most likely due to a deviation of the Tm sublattice magnetization from its easy direction, as indicated in diagram (b). At 22 T, a magnetization jump occurs from the configuration in diagram (b) to that in diagram (c). Above the jump, the two

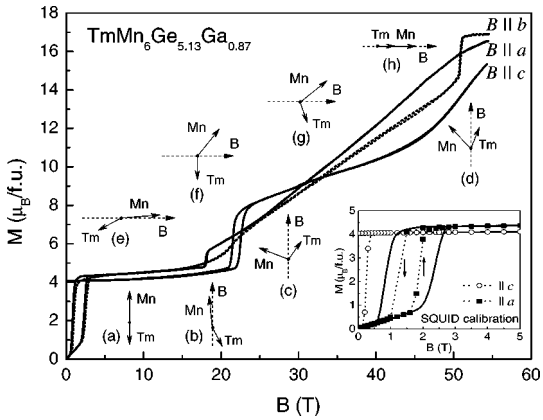

FIG. 12. Magnetization of TmM_6Ge$_{5.13}$Ga$_{0.87}$, measured at 4.2 K along the *a*-axis, the *b*-axis (dotted curve) and the *c*-axis. The inset shows SQUID measurements for calibration.

sublattice moments gradually bend further into the field direction as indicated in diagram (d). In the Tm compound, the magnetization jump occurs at a much lower field strength than in the Er compound where it is found at 32 T. This can be explained by the fact that the *R*-Mn intersublattice-coupling strength is weaker in the case of Tm than in the case of Er. The isotherm measured with the field applied in the hard magnetization direction, along the *a*-axis, initially has no spontaneous magnetization for *B* smaller than 1.5 T as shown in diagram (a). Increasing field yields an almost rigid rotation of both sublattices implying that anisotropy is probably weak. For field strengths between 2 and 18 T, the moment arrangement can be represented as shown in diagram (e). The total magnetization is slightly larger than that along the *c*-axis, because the slight deviation of the Tm moment is favored by the axial anisotropy of Tm. The jump in magnetization around 18 T can be interpreted as a jump of the Tm moment into a direction closer to the applied-field direction, retaining the anisotropy energy as far as possible at the cost of some of the antiferromagnetic intersublattice-coupling energy [diagram (f)]. The lower transition field compared to that along the *c*-axis indicates that the configuration in diagram (f) is favored by the axial anisotropy of the Tm sublattice. Above the magnetization jump the magnetization increases steadily as a consequence of further bending of the two sublattices towards each other [diagram (g)]. Along the *b*-axis, the jump around 20 T becomes less pronounced compared to the one in 18 T along the *a*-axis. The saturation magnetization is almost reached via a final jump in 50 T [diagram (h)], indicating a less strong Tm-Mn antiferromagnetic coupling compared to the other R-Mn compounds discussed here.

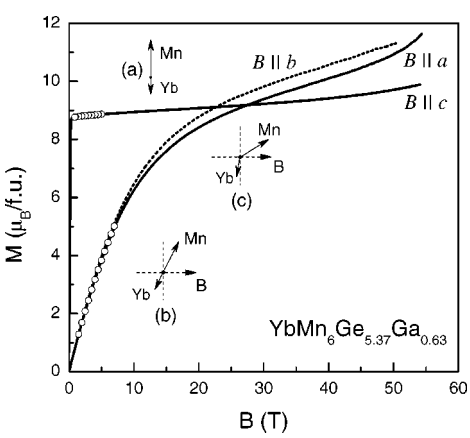

FIG. 13. Magnetization of YbMn$_6$Ge$_{5.37}$Ga$_{0.63}$, measured at 4.2 K along the *a*-axis, the *b*-axis (dotted curve) and the *c*-axis. The symbols represent SQUID measurements for calibration.

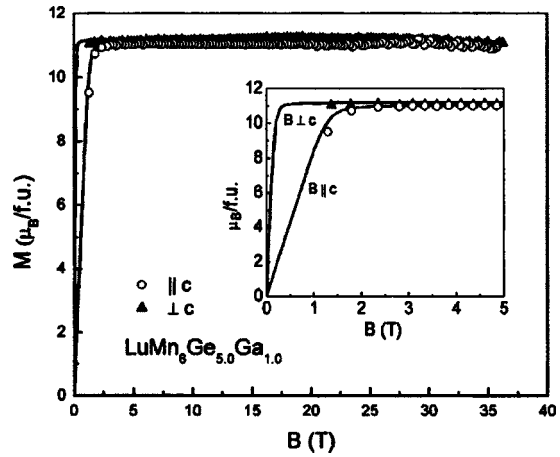

FIG. 14. Magnetization of LuMn$_6$Ge$_5$Ga, measured at 4.2 K along the *a*-axis and the *c*-axis. The solid lines represent SQUID measurements for calibration.

The results for the Yb compound are displayed in Fig. 13. When the field is applied in the *c* direction [diagram (a)], the easy magnetization direction, there is initially only a modest increase in magnetization. At higher fields up to 54 T, the slight upward curvature on magnetization may be indicative for the onset of a magnetization jump at a still higher field value. The isotherm for the hard magnetization direction (along the *a* direction) shows initially almost linear behavior, corresponding to a rigid rotation of the collinearly oriented Mn- and Yb-sublattice moments [diagram (b)]. Then, a bending process in the direction of the applied field prevails and the magnetization exhibits a sluggish increase [diagram (c)]. Also the high-field part of this isotherm suggests a jump of the magnetization to occur at a field value higher than applied in the present study. Along the *b*-axis, the magnetization has higher values than along the *a*-axis during the bending process. A catch-up occurred for the *a*-axis by the increase in slope above 50 T.

The results for the Lu compound are shown in Fig. 14. This ferromagnetic compound has its easy direction perpendicular to the *c* direction. For both applied-field directions, perpendicular and parallel to the *c*-direction, the magnetization saturates within the experimental accuracy at the same value. The value of the spontaneous magnetization is 11.15 μ_B/f.u., which corresponds with 1.86 μ_B/Mn atom.

IV. DISCUSSION

In the previous sections, we have shown that the magnetic properties of the RMn$_6$Ge$_{6-x}$Ga$_x$ compounds are strongly de-

pendent on the magnetic anisotropy. From the magnetic properties of the compounds formed with R=Y, Lu, Sc, and Gd, we derive that the Mn sublattice is ferromagnetic and has easy-plane anisotropy. We will tacitly assume that this type of Mn-sublattice anisotropy is maintained in compounds where also the R sublattice contributes to the anisotropy.

The contributions of the R sublattice are crystal-field induced and the first- and second-order anisotropy constants K_1^R and K_2^R- can be represented by the expressions

$$K_1^R = -3/2\alpha_J\langle r^2\rangle A_2^0\langle O_2^0\rangle - 5\beta_J\langle r^4\rangle A_4^0\langle O_4^0\rangle, \quad (1)$$

$$K_2^R = 35/8\beta_J\langle r^4\rangle A_4^0\langle O_4^0\rangle. \quad (2)$$

The thermal averages of the second- and fourth-order Stevens operators are represented by $\langle O_2^0\rangle$ and $\langle O_4^0\rangle$ and the corresponding crystal-field parameters are A_2^0 and A_4^0. For the various R elements considered in the present study, the second-order Stevens coefficients α_J are negative for R=Tb, Dy and Ho, and positive for R=Er, Tm and Yb. The fourth-order Stevens coefficients β_J are positive for R=Tb, Er and Tm and negative for R=Dy, Ho and Yb. Bearing in mind that the Mn-sublattice anisotropy consists predominantly of a contribution of the first-order anisotropy constant (see Table II) we can write for the total anisotropy constants K_1 and K_2:

$$K_1 = K_1^{\mathrm{Mn}} - 3/2\alpha_J\langle r^2\rangle A_2^0\langle O_2^0\rangle - 5\beta_J\langle r^4\rangle A_4^0\langle O_4^0\rangle, \quad (3)$$

$$K_2 = 35/8\beta_J\langle r^4\rangle A_4^0\langle O_4^0\rangle, \quad (4)$$

where K_1^{Mn} is negative (see Table II).

For positive values of K_1, one has uniaxial anisotropy. An easy cone is obtained when K_1 is negative and K_2 positive, satisfying the additional condition

$$0 < |K_1| < 2K_2. \quad (5)$$

At low temperatures, the R-sublattice anisotropy is much larger than the Mn-sublattice anisotropy and the moment directions are virtually controlled only by the former anisotropy. A satisfactory account for the observed behavior can be obtained if one assumes that A_2^0 and A_4^0 are both negative and their relative magnitudes are approximately given by the ratio A_2^0/A_4^0=6.7 . At low temperatures, the values of $\langle O_2^0\rangle$ and $\langle O_4^0\rangle$ can be approximated by using $J_z=J$ in the corresponding expressions. The signs of K_1 and K_2 obtained under these conditions by means of Eqs. (1) and (2) are presented in Table III. Since under these conditions also relation (5) is satisfied, this leads to an easy cone for the compounds with Ho and Dy. The remainder of compounds shows uniaxial behavior. The expected preferred moment directions presented in the last column of the table are in full agreement with the experimentally observed moment directions.

We will now turn to higher temperatures. It is well known that the thermal averages $\langle O_2^0\rangle$ and $\langle O_4^0\rangle$ decay rapidly with increasing temperature. In fact, their values decrease with increasing temperature proportional to a high power of the reduced R-sublattice magnetization, $[\mu_R(T)/\mu_R(0)]^n$, with n =3 and n=10 for the second-order and fourth-order term, respectively. The upshot is that at room temperature the anisotropy will be dominated by the Mn-sublattice contribution. The latter is of the easy plane type and differs from the preferred moment direction of the various RMn$_6$Ge$_{6-x}$Ga$_x$ compounds at low temperatures, which are either easy axis or easy cone. As a consequence, spin-reorientation transitions are expected to occur at some intermediate temperatures. Such transitions have been observed in all cases; see Table I.

TABLE III. Rare-earth contributions to the anisotropy in RMn$_6$Ge$_{6-x}$Ga$_x$ compounds at low temperature and moment arrangement to be expected if the R-sublattice anisotropy predominates.

R	K_1^R	K_2^R	Anistropy type
Tb	+	−	Easy axis
Dy	−	+	Easy cone
Ho	−	+	Easy cone
Er	+	−	Easy axis
Tm	+	−	Easy axis
Yb	+	+	Easy axis

V. CONCLUSIONS

We have studied the magnetic properties of single crystals of various RMn$_6$Ge$_{6-x}$Ga$_x$ compounds for x values close to one. Measurements made on the compounds in which the R component does not carry a magnetic moment reveal that the Mn sublattice orders ferromagnetically with a preferred moment direction perpendicular to the c-axis. When also the R component carries a magnetic moment, the latter couples antiparallel to the Mn moments and imposes a strong contribution to the total magnetocrystalline anisotropy upon cooling from room temperature to cryogenic temperatures. In all cases investigated, this leads to spin-reorientation transitions at intermediate temperatures. The dominance of the R-sublattice anisotropy at low temperatures leads to preferred moment directions characterized by an easy axis for R=Tb, Er, Tm and Yb and by an easy cone for R=Dy and Ho. Crystal-field theory has been used to give a satisfactory account of the observed phenomena. The magnetic properties of the RMn$_6$Ge$_{6-x}$Ga$_x$ compounds have been further characterized by measurements of the magnetization in high magnetic fields. Here, the interplay between the antiferromagnetic intersublattice R-Mn coupling and the magnetocrystalline anisotropy leads to pronounced field-induced magnetic phase transitions in the compounds with Dy, Ho, Er and Tm. A comparatively small in-plane anisotropy is revealed when comparing the high-field magnetization measurements along the a-axis with those along the b-axis.

ACKNOWLEDGMENTS

Some of the authors (L. Zhang, E. Brück) are grateful to the Dutch Technology Foundation STW for financial support.

[1] G. Venturini, R. Welter, and B. Malaman, J. Alloys Compd. **185**, 99 (1992).
[2] J. H. V. J. Brabers, V. H. M. Duijn, F. R. de Boer, and K. H. J. Buschow, J. Alloys Compd. **198**, 127 (1993).
[3] P. Schobinger-Papamantellos, G. André, J. Rodriguez-Carvajal, J. H. V. J. Brabers, and K. H. J. Buschow, J. Alloys Compd. **226**, 113 (1995).
[4] H. G. M. Duijn, E. Brück, K. H. J. Buschow, and F. R. de Boer, J. Magn. Magn. Mater. **196–197**, 691 (1999).
[5] M. T. Kelemen, P. Rösch, E. Dormann, and K. H. J. Buschow, J. Magn. Magn. Mater. **223**, 253 (2001).
[6] C. Lefèvre, G. Venturini, and B. Malaman, J. Alloys Compd. **337**, 1 (2002).
[7] C. Lefèvre, G. Venturini, and B. Malaman, J. Alloys Compd. **343**, 38 (2002).
[8] F. Canepa, M. Napoletano, C. Lefèvre, and G. Venturini, J. Alloys Compd. **339**, 26 (2002).
[9] C. Lefèvre, G. Venturini, and B. Malaman, J. Alloys Compd. **354**, 47 (2003).
[10] G. Venturini, A. Vernière, and B. Malaman, J. Alloys Compd. **320**, 46 (2001).
[11] W. Sucksmith and J. E. Thompson, Proc. R. Soc. London, Ser. A **225**, 362 (1954).